

# An aquifer thermal energy storage model for efficient simulations of district systems

Elisa Scalco <sup>a,b</sup>, Angelo Zarrella <sup>a</sup>, Alessandro Maccarini <sup>b</sup>, Alireza Afshari <sup>b</sup>

<sup>a</sup> Department of Industrial Engineering, University of Padova, Padova, Italy, elisa.scalco.2@studenti.unipd.it, angelo.zarrella@unipd.it.

<sup>b</sup> Department of the Built Environment, Aalborg University, Copenhagen, Denmark, amac@build.aau.dk, aaf@build.aau.dk.

**Abstract.** Thermal energy storage systems are valuable assets to enable high penetration of renewable energy sources into district heating and cooling (DHC) systems. One of the main benefits of using thermal storage is that it can contribute to matching energy supply and energy demand when they do not coincide in time.

Aquifer thermal energy storage (ATES) is an attractive technology to provide sustainable heating and cooling to buildings through DHC systems. In ATES systems, storage and recovery of thermal energy is achieved by extraction and injection of groundwater using wells. To calculate the energy performance of ATES, most of the studies use detailed simulation models developed using computational fluid dynamics software. However, such programs have limited capability of simulating the integration of ATES into building and district energy systems.

The aim of this research study is to develop a simplified ATES model, which is suitable for coupling with building and district energy simulation programs. The model has been developed using a finite-difference approach in the MATLAB computing platform to solve the transient heat and mass transfer equations in porous media in two dimensions. The aquifer around the wells is modelled as two independent radially symmetric discs with an inner radius and an outer radius. The model has been validated by comparing predicted warm/cold well temperatures with measurements data from literature. Since the model is developed in MATLAB, it can be coupled with building energy software (such as TRNSYS, Modelica, EnergyPlus) via co-simulation.

**Keywords.** ATES system, building energy simulation, MATLAB, thermal storage, district heating, district cooling.

**DOI:** <https://doi.org/10.34641/clima.2022.346>

## 1. Introduction

According to literature, the building sector has become the largest source of greenhouse gas (GHG) emissions and it is responsible of 40% of global energy consumption and one-third of global GHG emissions [1]. When considering residential buildings, space heating and space cooling represent the two most energy demanding end-uses [2]. Therefore, research in the field of efficient building energy systems is crucial to reduce the global GHG emissions and mitigate the effects of the climate change.

A large body of the literature has attempted to identify the main factors affecting the building sector's carbon emissions and Gholipour et al. [3]

concluded that the main drivers of buildings' CO<sub>2</sub> emissions and energy demand are income, energy price, and outdoor temperature, followed by population and heated floor area. Thermal energy is vital also for industry process that are usually very demanding, with most of the heat demand currently met through fossil-fuel based sources.

A more sustainable energy system requires the adoption of renewable energy, and in order to fill in the time gap between production and demand, thermal energy storage is a key solution. There are essentially four main groups: hot water thermal energy storage (HTES), gravel-water thermal energy storage (GWTES), borehole thermal energy storage (BTES) and aquifer thermal energy storage (ATES).

Thermal storage focuses on saving thermal energy that would otherwise be wasted. Guo et al. [4] studied a large-scale industrial waste heating system integrated with borehole thermal energy storage, running with temperatures above 200°C. Another example of underground large-scale thermal energy storage system was proposed by Zhou et al. [5] in China, whose energy demand has exceeded that of the United States [6] and where coal is still used with respiratory diseases reaching 30%. In this case it reveals that USTES (underground seasonal thermal energy storage) has significant economic, social and environmental benefits. However, large heat loss and low solar fraction are still common challenges for large-scale applications.

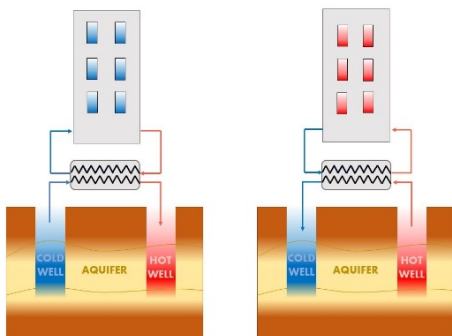


**Fig. 1** – Cooling and heating configuration in ATEs.

The low-grade waste heat is more suitable for district heating usage, due to its low exergy level. On a district level, ATEs systems are a very promising technology when it comes to tackle heating and cooling energy demand. They enable up to 40% of energy savings [7], by providing sustainable space cooling and space heating for buildings through seasonal storage of heat in already existing aquifers, underground layers of water-bearing permeable rock mixed with other materials such as gravel and sand. ATEs systems consist of at least two wells, a hot and cold one, used to either inject or withdrawal the groundwater. They usually work on a seasonal cycle. In winter, when heating mode is to be set, hot water is extracted from the hot well and is sent towards the internal heat exchanger of the building, that could be also provided with a heat pump to better adjust the temperatures needed by the users. The return cold water is sent towards the cold well to be stored for use in the following season when cooling mode will be needed. These systems though are not only meant for seasonal storage. As proved by De Schepper et al. [8] in the context of demand-side management and geothermal energy production also shorter frequencies of storage can provide good results.

As pointed out by Rostampour et al. [9] the spatial layout of ATEs systems is a key aspect for the technology, as thermal interactions between neighbouring systems can degrade the performances. Considering this issue, current planning policies for ATEs aim to avoid thermal interactions. However, under such policies, some urban areas already lack space for the further

development of ATEs, limiting achievable energy savings.

While these systems conventionally work on a range of 5-25°C and referred to as low temperature ATEs, high temperature ones (HT-ATEs) also exist and are gaining more and more attention by the research community thanks to their higher storage temperature, which can exceed 90°C. This enables the use of waste heat coming from a wider range of sources, such as CHP plants for example. With such temperatures, they could also provide energy for electricity generation baseload power. Organic Rankine cycle generators can use hot water between 80°C and 350°C, binary cycle geothermal power plants can exploit temperatures ranging from 70°C to 180°C, while flash steam power plants typically use hot water up to 300°C [10].

Unfortunately, when injecting warm/hot water there is a potential risk of minerals precipitation and also microorganisms' growth. The higher the operating temperature, more likely to be affected by this risk. HT-ATEs therefore are usually located in deeper aquifers to reduce this environmental impact, meaning the requirement of deeper drilling and so higher overall costs.

The main benefit of a higher fluid temperature is a higher energy density, and therefore higher economic benefits. As stated by Huang et al. [11] operating at higher temperatures could eliminate the need for the heat pump that raises the temperature of the fluid before it enters district heating networks, thereby reducing investment costs. One must also take into account that when increasing the storage temperature, the number of waste heat sources in fact increases but the overall storage efficiency decreases as more heat will be lost to the surroundings [7].

Finally, ATEs systems are widely recognized as a valuable solution for saving energy. Compared to traditional cooling/heating systems, about 90-95% of energy savings can be achieved when ATEs are used directly. When coupled with heat pumps, they can lead to about 60-85% of energy savings [12]. By using the available subspace in cities, these systems can be optimally linked and integrated on a urban level. As presented in a case study in Finland, the integration of ATEs systems with balanced pumping volumes in summer and winter with GWHP for DC and DH had a positive result in terms of system's efficiency, impact on the surrounding groundwater areas and techno-economic feasibility [13].

As in all systems, an evaluation of the thermal behaviour of an ATEs system is fundamental to improve the application and quantify the benefits. Common ATEs systems simulation models are for example MODFLOW or belong to the MT3D family [14]. They are finite-difference software that work on groundwater transport modelling and require groundwater flow equations solving. They mainly

focus on the aquifer itself, by working on its hydrogeologic characteristics and by the means of hydrogeologic boundaries. As anticipated in the abstract, the aim of this research study is to develop a simplified lumped-element model for ATEs systems that is capable of being connected and could properly work with building energy simulation programs at district level. To reach this result, a series of simplifications and assumptions have been made in order to develop a model that is simple, yet flexible enough for the purposes just mentioned but without affect the quality of the results.

## 2. Model description

### 2.1 Overview

Both wells have been considered as two independent cylinders for which the height has been initially set (coinciding with the ATEs thickness), together with the radius, beyond which an undisturbed ground temperature was considered. The first interest was studying the time and spatial variation of the temperature only on the radial direction, so an axial symmetry has been assumed, with the temperature kept constant along the depth of the aquifer,  $z$  direction in Fig. 2.

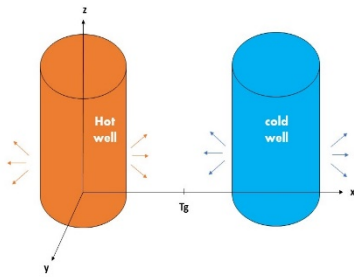


Fig. 2 - Hot and cold wells discretization.

As far as it concerns the methodology, the numerical model was developed in MATLAB and the starting point has been solving the transient heat and mass transfer equations in porous media in one dimension with a finite-difference approach.

### 2.2 Numerical model

A 1D discretization was considered to study how the temperature within the aquifer changes in the radial direction. To assess the behaviour of the aquifer, it was used a lumped-parameter system where for each node, representing a certain distance from the axis of the well, a thermal resistance and a thermal capacitance were assigned.

For the sake of simplicity, the following sections show the equations used in the model for a 3-node system.

### 2.3 1D model with heat conduction and heat advection

The following system consists of three active nodes, from 1 to 3, and two boundary conditions in node 0 (representing the bore wall) and node  $g$  at  $T_g$  (representing the undisturbed ground).

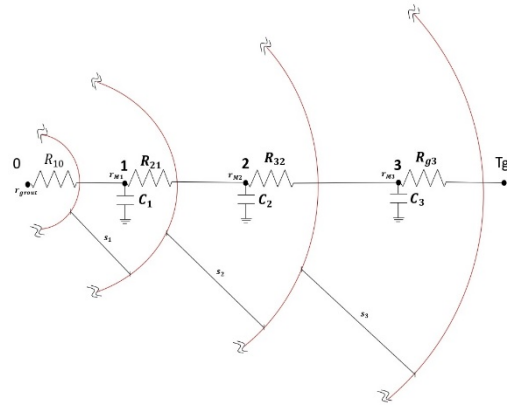


Fig. 3 - Lumped discretization for 3-node system.

For each thermal node (except the boundary conditions, nodes 0 and  $g$ ) there is a thermal resistance and a thermal capacitance. Each node with a lumped thermal capacitance is placed into the barycentric medium radius,  $r_M$ , of the corresponding annulus. Each annulus is spaced from the previous one according to an expansion coefficient  $c$ , that is arbitrary, and it is set at the beginning of the simulation. It is usually assumed between 1.1 and 1.2 and it is used to increase the thickness of the annulus starting from the grout radius. For example, for node 1:

$$s_1 = c * r_{grout} \quad (1)$$

$$r_{ext,1} = r_{grout} + s_1 \quad (2)$$

$$r_{M1} = \sqrt{\frac{r_{ext,1}^2 + r_{grout}^2}{2}} \quad (3)$$

For each node the energy balance equation was written, taking into account in this example just the heat conduction:

Node 1:

$$\frac{T_0^p - T_1^p}{R_{10}} + \frac{T_2^p - T_1^p}{R_{21}} = C_1 \frac{T_1^p - T_1^{p-1}}{\Delta\tau} \quad (4)$$

Node 2:

$$\frac{T_1^p - T_2^p}{R_{21}} + \frac{T_3^p - T_2^p}{R_{32}} = C_2 \frac{T_2^p - T_2^{p-1}}{\Delta\tau} \quad (5)$$

Node 3:

$$\frac{T_g^p - T_3^p}{R_{g3}} + \frac{T_2^p - T_3^p}{R_{32}} = C_3 \frac{T_3^p - T_3^{p-1}}{\Delta\tau} \quad (6)$$

For each active node there are three contributions. A heat conduction flow for each surrounding node (on the left side of the equation) and the contribution due to the stored heat (on the right side of the equation), expressed through the thermal capacitance.

In Equations (4-6) the superscripts “p-1” and “p” indicate the time dependence of the equations. The finite difference solution restricts the temperature to discrete points (nodes) in space but also in time. In fact, calculations were made at successive times, each one separated by a certain time step,  $\Delta\tau$ , set by the user. So that:

$$t = p\Delta\tau \quad (7)$$

Therefore, the calculation starts at time “p-1” for a generic  $n$  node, the input system will be  $T_n^{p-1}$  and the output will be the temperature at the current time,  $T_n^p$ .

When working with an ATES, there are three distinct phases. First the system is charged with a certain water flow, this is the injection period. Once the ATES is charged it will have reached a certain temperature, this is the storage period. Finally, when it needs to be activated, the water flow will be extracted and sent to the complex of buildings, this is the withdrawal period.

The next step deals with a water flow to essentially model the injection and withdrawal phases.

During the injection phase a certain water flow is being injected into the aquifer through the grout at a certain known temperature.

With **Fig. 3** as reference, these are the correlated equations:

Node 1:

$$\frac{T_0^p - T_1^p}{R_{10}} + \frac{T_2^p - T_1^p}{R_{21}} + \rho c_p \dot{V} (T_0^p - T_1^p) = C_1 \frac{T_1^p - T_1^{p-1}}{\Delta\tau} \quad (8)$$

Node 2:

$$\frac{T_1^p - T_2^p}{R_{21}} + \frac{T_3^p - T_2^p}{R_{32}} + \rho c_p \dot{V} (T_1^p - T_2^p) = C_2 \frac{T_2^p - T_2^{p-1}}{\Delta\tau} \quad (9)$$

Node 3:

$$\frac{T_g^p - T_3^p}{R_{g3}} + \frac{T_2^p - T_3^p}{R_{32}} + \rho c_p \dot{V} (T_2^p - T_3^p) = C_3 \frac{T_3^p - T_3^{p-1}}{\Delta\tau} \quad (10)$$

During the storage phase there is no water flow involved, as the system is still. Therefore, it is ascribable to the model here presented.

Finally, when it comes to the withdrawal, the system works in reverse compared to the injection. The water flow then will stream in the other direction. This time though the withdrawal temperature,  $T_o$ , is unknown.

Still referencing to **Fig. 3**:

Node 0:

$$\frac{T_1^p - T_0^p}{R_{10}} + \rho c_p \dot{V} (T_1^p - T_0^p) = 0 \quad (11)$$

Node 1:

$$\frac{T_0^p - T_1^p}{R_{10}} + \frac{T_2^p - T_1^p}{R_{21}} + \rho c_p \dot{V} (T_2^p - T_1^p) = C_1 \frac{T_1^p - T_1^{p-1}}{\Delta\tau} \quad (12)$$

Node 2:

$$\frac{T_1^p - T_2^p}{R_{21}} + \frac{T_3^p - T_2^p}{R_{32}} + \rho c_p \dot{V} (T_3^p - T_2^p) = C_2 \frac{T_2^p - T_2^{p-1}}{\Delta\tau} \quad (13)$$

Node 3:

$$\frac{T_g^p - T_3^p}{R_{g3}} + \frac{T_2^p - T_3^p}{R_{32}} + \rho c_p \dot{V} (T_g^p - T_3^p) = C_3 \frac{T_3^p - T_3^{p-1}}{\Delta\tau} \quad (14)$$

To sum up:

- Storage and injection systems working with  $n$  nodes will require solving  $n$  equations.
- Withdrawal system working with  $n+1$  nodes will require solving  $n+1$  equations.

## 2.4 2D model with heat conduction and heat advection

The following step focuses on the modelling of the upper and lower layers of the aquifer. This meant studying not only the radial direction, but also the vertical one.

As it can be seen in **Fig. 4**, two layers (above and below) have been added to the pre-existent aquifer model. This new space discretizes the ground adjacent to the aquifer. To keep the model simple enough, a limited number of nodes have been added, where only heat conduction takes place.

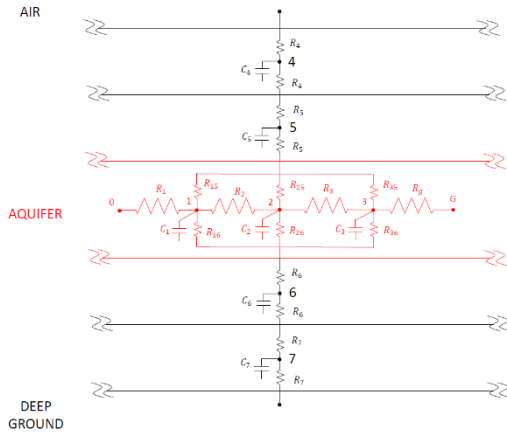


**Fig. 4** – Final discretized ground.

Compared to the previous situation, heat conduction through these new layers has been added (in the vertical direction) in each thermal balance equation.

Still referencing to **Fig. 4**, during the injection phase:

Node 4

$$\frac{T_{air}^p - T_4^p}{R_4} + \frac{T_5^p - T_4^p}{R_4 + R_5} = \frac{C_4(T_4^p - T_4^{p-1})}{\Delta\tau} \quad (15)$$

Node 5:

$$\frac{T_5^p - T_4^p}{R_4 + R_5} + \frac{T_1^p - T_5^p}{R_{15} + R_5} + \frac{T_2^p - T_5^p}{R_{25} + R_5} + \frac{T_3^p - T_5^p}{R_{35} + R_5} = \frac{C_5(T_5^p - T_5^{p-1})}{\Delta\tau} \quad (16)$$

Node 1:

$$\frac{T_0^p - T_1^p}{R_1} + \frac{T_2^p - T_1^p}{R_2} + \rho c_p \dot{V}(T_0^p - T_1^p) + \frac{T_5^p - T_1^p}{R_{15} + R_5} + \frac{T_6^p - T_1^p}{R_{16} + R_6} = \frac{C_1(T_1^p - T_1^{p-1})}{\Delta\tau} \quad (17)$$

Node 2:

$$\frac{T_1^p - T_2^p}{R_2} + \frac{T_3^p - T_2^p}{R_3} + \rho c_p \dot{V}(T_1^p - T_2^p) + \frac{T_5^p - T_2^p}{R_{25} + R_5} + \frac{T_6^p - T_2^p}{R_{26} + R_6} = \frac{C_2(T_2^p - T_2^{p-1})}{\Delta\tau} \quad (18)$$

Node 3:

$$\frac{T_2^p - T_3^p}{R_2} + \frac{T_4^p - T_3^p}{R_3} + \rho c_p \dot{V}(T_2^p - T_3^p) + \frac{T_5^p - T_3^p}{R_{35} + R_5} + \frac{T_6^p - T_3^p}{R_{36} + R_6} = \frac{C_3(T_3^p - T_3^{p-1})}{\Delta\tau} \quad (19)$$

Node 6:

$$\frac{T_7^p - T_6^p}{R_6 + R_7} + \frac{T_1^p - T_6^p}{R_{16} + R_6} + \frac{T_2^p - T_6^p}{R_{26} + R_6} + \frac{T_3^p - T_6^p}{R_{36} + R_6} = \frac{C_6(T_6^p - T_6^{p-1})}{\Delta\tau} \quad (20)$$

Node 7:

$$\frac{T_{ground}^p - T_7^p}{R_7} + \frac{T_6^p - T_7^p}{R_7 + R_6} = \frac{C_7(T_7^p - T_7^{p-1})}{\Delta\tau} \quad (21)$$

To each new node a new equation has been added, alongside with two new boundary conditions, the air temperature above and the deep ground temperature below.

For the aquifer nodes (1 to 3) there is the new contribution of heat conduction due to node 5 and node 6.

During the withdrawal phase as shown before there will be an additional equation related to node 0.

### 3. Model validation

The final step has been validating the model. To do so data from a research paper by Carotenuto et al. [15] has been used as reference. In this paper, an ATEs system placed in Capua (Italy) was studied and tested. The experiment consisted of charging the aquifer, storing the heat and then withdrawing the water flow. **Fig. 5** outlines the aquifer located at 42 m underground. It is described as coarse sandy and gravelly.

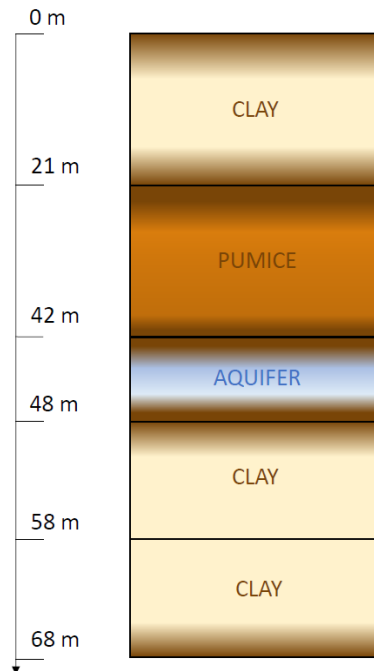


**Fig. 5** – Simplified stratigraphy section of the case study.

The experiment was based on two wells (W1, W2). During the injection phase the water flow was

pumped into W1, after been heated, and following the storage period was pumped back into W2. The experiment was carried out during July and August of 1990 in the following way:

- a 34 m<sup>3</sup>/h water flowrate at 16°C was pumped from W2, heated via a plate heat exchanger up to 40°C and finally injected into W1. After a period of settlement, this water flow was extracted and pumped back into W2.
- The injection period lasted 15 days, the storage 7 days and 15 hours and the withdrawal another 15 days.

**Tab. 1** and **Tab. 2** describe all the input data that has been used to run the simulation.

In order to validate the model, simulation results have been compared to measured temperature data provided by the paper. **Fig. 6** shows the three different trends.

**Tab. 1** – Thermophysical properties

layer	cv	λ
	[J/(m <sup>3</sup> K)]	[W/(m K)]
Pumice	2.4·10 <sup>6</sup>	1
Aquifer	2.6·10 <sup>6</sup>	1.3
Clay	2.3·10 <sup>6</sup>	0.8

**Tab. 2** – Boundary Temperatures

Node	T
	°C
Air	10
(Deep) Ground	16
Aquifer	16
(Aquifer) Ground	16
Grout	40

The yellow curve is the data related to the actual measured temperature on the site during the experiment. This is the average temperature measured by three thermocouples positioned in the aquifer at 46.5, 45.0 and 42.5 m of depth. The green curve is the temperature trend as result of the 1-dimensional model simulation while the brown one is the 2-dimensional one.

Before the first phase, the temperature node (placed at 10 m from the well) is at 16°C. Once the injection starts, a hot water flow (around 40°C) is pumped into

the well and the node temperature slowly increases, reaching the set point after 100 hours (about 4 days). During this phase, the two simulations provide results quite alike because the vertical heat conduction is negligible. Compared to the yellow curve, the simulated aquifer is in both cases a bit slow during this charge. The little stall in the yellow curve after 40 hours and again after 100 hours could be related to some measuring error. Injection finishes after 360 hours.

During the storage phase the two models start to differentiate from each other. This is where the vertical heat losses come into play. Given that the aquifer has a temperature of 40°C, the ΔT between the aquifer and the other layers is now large enough that vertical heat conduction becomes relevant.

Finally, in the withdrawal phase, the 2D simulation model shows better results in comparison to the 1D simulation model. The 2D aquifer compared to experimental data is quite slow in this final phase. This effect could be due to the groundwater leaks that are not considered in the model.

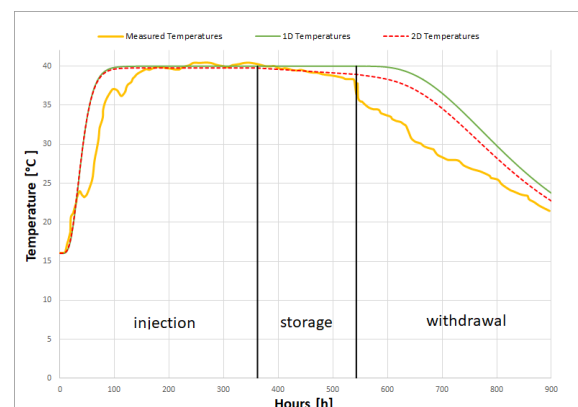


**Fig. 6** – Average temperatures plotted vs time at 10 m from W1

## 4. Conclusions

This work presented a first approach for a simplified model to evaluate the thermal behavior and application of ATEs in design planning. The model was based on a lumped parameter approach and was compared with measurements presented in literature. Despite the simplifications, the model for a single well has proved itself to work fine and give good enough results in terms of temperatures. The interaction between adjacent wells will be the future aspect that will be considered. The key feature of the model is its ability to be linked to building and district simulation tools. This feature will be further implemented in the future in order to evaluate the benefits of ATEs in different contexts.

## 5. Data availability

The datasets generated during and/or analyzed during the current study are not publicly available because measurements were not carried out by the Authors but are/will be available upon request

## 6. Acknowledgements

This work was supported by the Danish Energy Agency, under the Energy Technology Development and Demonstration Program (EUDP), journal no. 64019-0575.

This research emerged from the Task 32 project; an international project conducted under the umbrella of the International Energy Agency (IEA) within Energy Storage Technology Collaboration Programme (ES TCP).

## 7. Nomenclature

C thermal capacitance [ J/K ]

$c_v$  volume specific capacity [ J/(m<sup>3</sup>K) ]

$c_p$  thermal specific capacitance [ J/ (kg K) ]

c expansion coefficient [-]

$\lambda$  thermal conductivity [ W/ (m K) ]

$\Delta\tau$  time step [ s ]

$r_M$  barycentric medium radius [ m ]

$\rho$  density [ kg/m<sup>3</sup> ]

R thermal resistance [ K/W ]

$r_i$  annulus radius [ m ]

s annulus thickness [ m ]

t time [ s ]

T temperature [ °C ]

V volumetric water flow [ m<sup>3</sup>/s ]

*Subscripts and superscripts*

p: time instant

g: aquifer ground

## 8. References

[1] Yang T., Pan Y., Yang Y., Lin M., Qin B., Xu P., Huang Z. CO<sub>2</sub> emissions in China's building sector through 2050: A scenario analysis based on a bottom-up model. 2017,06,1;

[2] Bloemendal M., Jaxa-Roxen M., Olsthoorn T. Methods for planning of ATEs systems. 2018,2,22;

[3] Gholipour H., Arjomandi A., Yam S. Green property finance and CO<sub>2</sub> emissions in the building industry. 2022,2;

[4] Guo F., Zhu X., Li P., Yang X. Low-grade industrial waste heat utilization in urban district heating: Simulation-based performance assessment of a seasonal thermal energy storage system. 2022,1,15;

[5] Zhou X., Xu Y., Zhang X., Xu D., Linghu Y., Guo H., Wang Z., Chen H. Large scale underground seasonal thermal energy storage in China. 2021,1;

[6] Wilberforce T., Olabi A., Sayed E., Elsaid K., Maghrabie H.M., Abdelkareem M. A review on zero energy buildings – Pros and cons. 2021,07,24;

[7] Mahon H., O'Connor D., Friedrich D., Hughes B. A review of thermal energy storage technologies for season loops. 2021,9,28;

[8] De Schepper G., Paulus C., Bolly PY., Hermans T., Lesparre N., Robert T. Assessment of short-term aquifer thermal energy storage for demand-side management perspectives: Experimental and numerical developments. 2019,05,15;

[9] Rostampour V., Jaxa-Rozen M., Bloemendal M., Kwakkel J., Keviczky T. Aquifer Thermal Energy Storage (ATES) smart grids: Large-scale seasonal energy storage as a distributed energy management solution. 2019,05,15;

[10] Heather A. Sheldon, Andy Wilkins, Christopher P. Green. Recovery efficiency in high-temperature aquifer thermal energy storage systems. 2021,11;

[11] Huang Y., Pang Z., Kong Y., Watanabe N. Assessment of the high-temperature aquifer thermal energy storage (HT-ATES) potential in naturally fractured geothermal reservoirs with a stochastic discrete fracture network model. 2021,12;

[12] Bozkaya B., Li R., Labeodan T., Kramer R., Zeiler W. Development and evaluation of a building integrated aquifer thermal storage model. 2017,6,28;

[13] Todorov O., Alanne K., Virtanen M., Kosonen R. A method and analysis of aquifer thermal energy storage (ATES) systems for district heating and cooling: A case study in Finland. 2019,9,20;

[14] MODFLOW  
<https://www.usgs.gov/software/modflow-6->

usgs-modular-hydrologic-model

- [15] Carotenuto A, Fucci F, La Fianza G, Reale F. Physical model and demonstration of an aquifer thermal energy store. 1991,11(2-3):169:180;